DOI: 10.1478/AAPP.1011A10

AAPP | Atti della Accademia Peloritana dei Pericolanti
Classe di Scienze Fisiche, Matematiche e Naturali
ISSN 1825-1242

Vol. 101, No. 1, A10 (2023)

NUMERICAL PERFORMANCE USING THE NEURAL NETWORKS TO SOLVE THE NONLINEAR BIOLOGICAL QUARANTINED BASED COVID-19 MODEL

ZULQURNAIN SABIR [a], MUHAMMAD ASIF ZAHOOR RAJA [b],
HACI MEHMET BASKONUS [c] AND ARMANDO CIANCIO [d*]

ABSTRACT. The current study provides the solutions of the mathematical model based on the coronavirus including the effects of vaccination and quarantine. The numerical stochastic process relying on Levenberg-Marquardt backpropagation technique (L-MB) neural networks (NN), i.e., L-MBNNs, is presented to solve the model. The entire dynamics of the proposed model depends upon the human population, which is represented by N and is further divided into multiple subgroups. The detail of these subgroups is presented in the form of susceptible population (S), exposed population (E), and infected people (I). Likewise, Q represents the quarantined and R shows the recovered or deceased individuals. Those who have been immunized are symbolized by V. All these categories make the model SEIQRV, that is based on a system of nonlinear differential equations. The statistics that is used to provide the numerical solutions of the SEIQRV model is 76% for training, 10% for testing and 14% for authorization. The correctness of the L-MBNNs is tested by using the comparison of the proposed and reference solutions (Adam method). The statistical representations are provided in order to check the reliability, competence and validity of L-MBNNs using the procedures of error histograms (EH), state transitions (ST), regression and correlation.

1. Introduction

Coronavirus is one of the dangerous and fastest spreading infectious diseases which the entire world was faced with at different levels. Coronaviruses are hypothesized to be a member of the viral family that infects both birds and mammals. Coronaviruses, at either end of the spectrum, produce mild respiratory duct disorders in humans. Based on the common cold, several diseases have been found including SARS, MERS, and coronavirus. It is critical to observe the classification of these viruses, which may frequently produce a risk to the community.

It is established that coronaviruses may cause bacterial or viral indirect or direct pneumonia. The most recent version of coronavirus is 2019-nCoV, produced through bats. However, there are various related theories that have been presented to its spreading. When such a virus is assumed to have originated via bats, the first question that arises is whether these

bats are new to our planet, and if not, why such a virus has not been produced before. Is it acceptable to claim that the lethal virus has never come into contact with humans? Because it was feared that such a virus had infected humans, white people began to ingest infected bats.

Coronavirus COVID-19 is caused by acute respiratory syndrome coronavirus 2 (SARS-CoV-2). COVID-19 shows global healthcare threat, with extremely fast geographical dissemination. Proactive strategies, especially conjunction with adequate sickness separation as well as population containment is necessary to reduce the high contagious public dissemination. The development of the vaccine used to eliminate the virus was studied by Umakanthan *et al.* (2020). COVID-19 reportedly infected millions of people around the entire globe with higher death ratio (Kumar *et al.* 2021). There are various investigations based on different drugs using the vaccine manufacture along with several pharmaceuticals (see Table 1) (Amawi *et al.* 2020).

SARS-CoV-2, which is highly contagious in humans and has transmitted rapidly over the globe by close human interaction or the spilling of contaminated persons' coughs and sneezes, is initially found in China (Wuhan city). Because of the increasing transmission in China, WHO declared the COVID-19 disease a "pandemic". COVID-19 seems to be a coronavirus species that corresponds to the Sarbecovirus subfamily, which contains several additional varieties to produce the extreme human disorders (Yüce, Filiztekin, and Özkaya 2021). Four basic elements present in the coronavirus are genetic structure (S), envelope (E), membrane (M), nucleocapsid (N), and spike (S). S, E, M, as well as N proteins seem to be virulent factors that are used in the reproduction of DNA. The rapidly spreading proteins are the human cell, which has attached the human angiotensin-converting enzyme 2 (ACE2) target. Consequently, those viral proteins potentially applied to the process of healing using the inhibit virus replication (Ao *et al.* 2020).

Differential equations provide the simulations of the dynamical phenomena in a wide range of disciplines, particularly fluid mechanics, epidemiology and engineering (Z. Ahmad *et al.* 2020a,b; N. Khan *et al.* 2021). The use of computational techniques in epidemiology is now common and has been a hot issue in various methodologies, which are used to describe and understand the patterns of contagious diseases (Martcheva 2015; Brauer 2017; A. Ciancio and Flora 2017; Agusto and M. A. Khan 2018; Ullah, M. A. Khan, and Farooq 2018; M. A. Khan and Atangana 2019; Ali *et al.* 2020; Sinan *et al.* 2022; A. Ciancio, V. Ciancio, and Flora 2023). Furthermore, the concept of optimum management has been used in the mathematical frameworks, which provides the avoidance of several pandemics in different areas with different periods (Sharomi and Malik 2017; Kantner and Koprucki 2020). Scientific research using the dynamics of several infectious illnesses is applied (Peter *et al.* 2021; Qureshi and Jan 2021). The fractional mathematical paradigms have been applied by Qureshi and Jan (2021) who examined the spread of measles in the human community. They studied and verified the findings through the actual data based on WHO. Memory is a strategy that has already been demonstrated to employ the fractional order structures (W. M. Ahmad and El-Khazali 2007; Song, Xu, and Yang 2010).

The existence of various scientific models may be regulated by using the power law, while others employ the Mittag-Leffler as well as exponential decay rules. To interpret the numerous fractional derivatives, Atangana (2017) initiated the groundbreaking differentiation operators. One of the novel operators is called fractal-fractional (FF) derivative,

which incorporates the fFF differentiation by using the revolutionary concepts of chaos, chemical activities, complicated dynamical processes and electrical circuits (Atangana 2017; Z. Ahmad *et al.* 2021).

In this study, the stochastic process Levenberg-Marquardt backpropagation technique (L-MB) neural networks (NNs), i.e., L-MBNNs, is presented to solve the model. The entire dynamics of the proposed model depends upon the human population presented by N, which is further divided into multiple subgroups. The detail of these subgroups is presented using the susceptible population S, exposed population E, and infected people I. Similarly, Q represents the quarantined and R shows the recovered or deceased individuals. Those who have been immunized are symbolized by V. All these categories make the model SEIQRV, which is based on a system of nonlinear differential equations.

The remaining part of the paper is divided into the following sections. In Sect. 2 we design a structure of the SEIQRV differential system for the COVID-19 with quarantine and vaccination. Section 3 provides new topographies for such differential systems using a COVID-19 SEIQRV model, providing a brief overview of stochastic solvers as well as essential novel characteristics of the L-MBNNs. Section 4 explains the construction of L-MBNNs. Section 5 contains the outcomes and simulations achieved using the proposed strategy for the SEIQRV model. The conclusions are discussed in Section 6.

2. Model development

Millions of deaths due to coronavirus have been reported in the world. It is stated that populations in isolation and the limitation can decrease the positive cases of coronavirus. Both isolation and restriction have been identified as effective measures for the elimination of this virus. As a result, the model examined below focuses on the entire propagation features of the novel coronavirus (2019-nCoV), including an investigation of quarantine and clinical isolation for the patients, who have been infected.

The current model is used to predict the spread of COVID-19 in the human population. The whole human population is indicated by $\mathscr{N}(\tau)$, which has been subdivided into multiple subcategories, i.e., the overall susceptible population is reflected via $\mathscr{S}(\tau)$, the exposing population is portrayed by $\mathscr{E}(\tau)$, and the infected people are depicted by $\mathscr{I}(\tau)$. Likewise, $\mathscr{Q}(\tau)$ denotes those who have been quarantined, while $\mathscr{R}(\tau)$ denotes those who have been recovered or removed/deceased. Individuals who have been vaccinated are represented by the character $\mathscr{V}(\tau)$. The process flow for such explored scenario is shown in Fig. 1, in which susceptible individuals could contact of $\mathscr{I}(\tau)$ via channel $\theta\mathscr{S}\mathscr{I}$ and get exposed. Some vulnerable persons are immunized having a vaccination rate of ϕ and, therefore, are classified as vaccination category $\mathscr{V}(\tau)$.

Considering susceptible people are more infectable, we evaluated only the vaccination of susceptible participants. People who have been exposed or infected have essentially been accustomed with the virus's activity and appearance, and therefore antibodies become highly effective compared to those who are vulnerable. As a result, we decided to postpone the immunization of these courses until time becoming. Identically, with an infection rate of η, affected individuals complete their incubation time and acquire the infectious class $\mathscr{I}(\tau)$. Furthermore, some infected people will recover or die as a result of the virus including a positive rate ς, whereas others will be quarantined having a positive rate φ. Finally, the

remaining quarantined persons are either retrieved or discarded owing to sickness at a rate of μ. Γ represents the natural death rate for all classes, whereas Γ represents the recruitment rate rather than the birth rate. The following list describes the parameters with description.

Parameter	Description	Dimension/ Unit
θ	Interaction rate between infected and susceptible individuals	Time^{-1}
η	Incubation period	Time^{-1}
φ	Quarantined rate of infected individuals	Time^{-1}
ϕ	Vaccination rate of susceptible individuals	Time^{-1}
ς	Recovery or removal rate of infected individuals	Time^{-1}
μ	Recovery or removal rate of quarantined individuals	Time^{-1}
Γ	recruitment rate	Population/ Time
γ	Natural mortality rate	Population/ Time

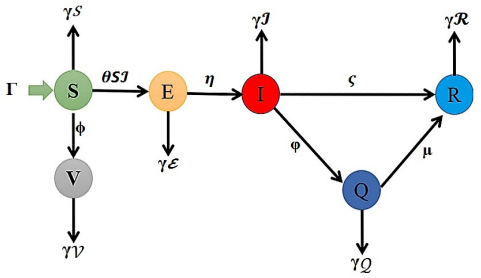

FIGURE 1. The model's process diagram.

The process flow of the studied model for COVID-19 occurrence is as follows: the combination of equations addressing the problem under consideration with non-negative IC's has been provided as

$$\begin{cases} \left(\dfrac{d\mathscr{S}}{d\tau}\right) = \Gamma - \theta\mathscr{S}\mathscr{I} - (\phi+\gamma)\mathscr{S}, \\ \left(\dfrac{d\mathscr{E}}{d\tau}\right) = \theta\mathscr{S}\mathscr{I} - (\eta+\gamma)\mathscr{E}, \\ \left(\dfrac{d\mathscr{I}}{d\tau}\right) = \eta\mathscr{E} - (\varphi+\varsigma+\gamma)\mathscr{I}, \\ \left(\dfrac{d\mathscr{Q}}{d\tau}\right) = \varphi\mathscr{I} - (\mu+\gamma)\mathscr{Q}, \\ \left(\dfrac{d\mathscr{R}}{d\tau}\right) = \varsigma\mathscr{I} + \mu\mathscr{Q} - \gamma\mathscr{R}, \\ \left(\dfrac{d\mathscr{V}}{d\tau}\right) = \phi\mathscr{S} - \gamma\mathscr{V}, \end{cases} \tag{1}$$

with

$$\begin{cases} \mathscr{S}(0) = \mathscr{S}^* \geq 0, \mathscr{E}(0) = \mathscr{E}^* \geq 0, \mathscr{I}(0) = \mathscr{I}^* \geq 0, \\ \mathscr{Q}(0) = \mathscr{Q}^* \geq 0, \mathscr{R}(0) = \mathscr{R}^* \geq 0, \mathscr{V}(0) = \mathscr{V}^* \geq 0. \end{cases}$$

3. Innovative topographies including an overview of stochastic solvers

Mathematical stochastic operations through L-MBNNs are introduced to solve SEIQRV based on the COVID-19 system. The local and global stochastic operators have already been used to address the wider range of nonlinear and complicated systems using the stochastic computing procedures (Sabir *et al.* 2021b, 2022). Moreover, the fractional order singular models have also been discussed by using the proposed schemes (Sabir, Guirao, and Saeed 2021; Sabir *et al.* 2021a). Moreover, the functional form of the differential models (Sabir *et al.* 2021a), Emden-Fowler delay differential model (Guirao, Sabir, and Saeed 2020) and periodic differential system (Sabir, Guirao, and Saeed 2021) and some other stiff models (Ghanbari and Djilali 2020; Sabir *et al.* 2020) have also been discussed by using the stochastic schemes. The purpose of this study is to present the numerical representations of SEIQRV based on the coronavirus differential system using the stochastic L-MBNNs technique.

The L-MBNNs with this differential system using the SEIQRV COVID-19 scheme appear to have the following major new properties:

- The nonlinear model based on SEIQRV using the dynamics of COVID-19 is numerically stimulated by using the proposed scheme.
- The first order derivatives of SEIQRV COVID-19 scheme that relies upon SEIQRV impacts are demonstrated to be successful in numerical investigations utilizing the stochastic scenarios.
- The nonlinear first order derivatives of the SEIQRV based COVID-19 system are solved using AI, which depends on the structure of L-MBNNs.
- To test the suggested scheme's dependability, three relevant first order variations of the SEIQRV based COVID-19 system were numerically solved.
- Through evaluating the manufactured and reference (Adam method) solutions, magnificence of stochastic computation solver-based L-MBNNs has been proven.
- Negligible absolute error (AE) results perform the correctness of the proposed stochastic scheme.
- The reliability of the stochastic L-MBNNs' approach is observed through the designed scheme along with the statistical performances of the regression, STs, EHs, and correlated values.

4. Methodological proposal: L-MBNNs

The L-MBNNs stochastic framework has been suggested in this study to solve the coronavirus model including the quarantine and vaccine impacts, called SEIQRV system. For the solutions of this model, the scheme performances are implemented in the form of stochastic operators and its implementations.

Figure 2 depicts a single-layer neuron arrangement as well as a multi-layer optimization strategy based on numerical stochastic L-MBNNs. The L-MBNNs processes are supplied in Matlab via the '$nftool$ function, with data such as 76% in training, 10% in testing, and 14% for authorisation stated.

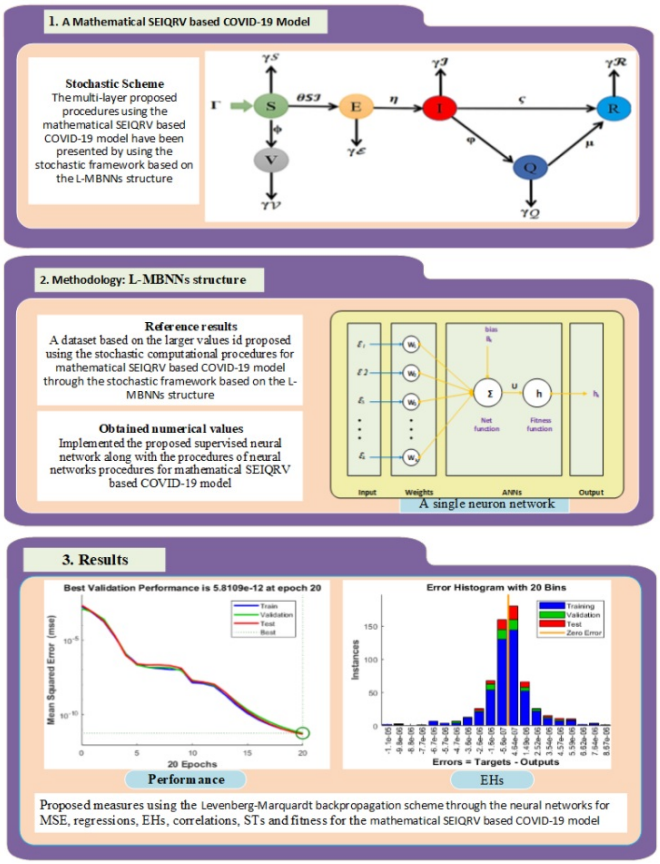

FIGURE 2. L-MBNNs workflow procedure to solve COVID-19 SEIQRV related model along with the formation of a single neuron.

5. Overall conclusions achieved by using the proposed approach

This phase shows numerical results with three different alternative changes to solve the SEIQRV COVID-19 system utilising recommended L-MBNNs. The differential description of each variation is presented in the scenario that follows.

Case 1

Implement the SEIQRV COVID-19 associated model with the given values ($\Gamma = 0.1,\ \theta = 0.15,\ \phi = 0.16,\ \gamma = 0.18,\ \eta = 0.2,\ \varphi = 0.22,\ \varsigma = 0.17,\ \mu = 0.25$):

$$\begin{cases} \left(\frac{d\mathscr{S}}{d\tau}\right) = 0.1 - 0.15\mathscr{S}\mathscr{I} + 0.02\mathscr{S}, & \mathscr{S}_0 = 0.10, \\ \left(\frac{d\mathscr{E}}{d\tau}\right) = 0.15\mathscr{S}\mathscr{I} - 0.02\mathscr{E}, & \mathscr{E}_0 = 0.12, \\ \left(\frac{d\mathscr{I}}{d\tau}\right) = 0.2\mathscr{E} - 0.57\mathscr{I}, & \mathscr{I}_0 = 0.14, \\ \left(\frac{d\mathscr{Q}}{d\tau}\right) = 0.22\mathscr{I} - 0.43\mathscr{Q}, & \mathscr{Q}_0 = 0.16, \\ \left(\frac{d\mathscr{R}}{d\tau}\right) = 0.17\mathscr{I} + 0.25\mathscr{Q} - 0.18\mathscr{R}, & \mathscr{R}_0 = 0.18, \\ \left(\frac{d\mathscr{V}}{d\tau}\right) = 0.16\mathscr{S} - 0.18\mathscr{V}, & \mathscr{V}_0 = 0.20. \end{cases} \tag{2}$$

Case 2

Employ the SEIQRV COVID-19 associated model with the appropriate values ($\Gamma = 0.1,\ \theta = 0.15,\ \phi = 0.16,\ \gamma = 0.18,\ \eta = 0.2,\ \varphi = 0.22,\ \varsigma = 0.17,\ \mu = 0.25$):

$$\begin{cases} \left(\frac{d\mathscr{S}}{d\tau}\right) = 0.1 - 0.15\mathscr{S}\mathscr{I} + 0.02\mathscr{S}, & \mathscr{S}_0 = 0.12, \\ \left(\frac{d\mathscr{E}}{d\tau}\right) = 0.15\mathscr{S}\mathscr{I} - 0.02\mathscr{E}, & \mathscr{E}_0 = 0.14, \\ \left(\frac{d\mathscr{I}}{d\tau}\right) = 0.2\mathscr{E} - 0.57\mathscr{I}, & \mathscr{I}_0 = 0.16, \\ \left(\frac{d\mathscr{Q}}{d\tau}\right) = 0.22\mathscr{I} - 0.43\mathscr{Q}, & \mathscr{Q}_0 = 0.18, \\ \left(\frac{d\mathscr{R}}{d\tau}\right) = 0.17\mathscr{I} + 0.25\mathscr{Q} - 0.18\mathscr{R}, & \mathscr{R}_0 = 0.20, \\ \left(\frac{d\mathscr{V}}{d\tau}\right) = 0.16\mathscr{S} - 0.18\mathscr{V}, & \mathscr{V}_0 = 0.22. \end{cases} \tag{3}$$

Case 3

Employ the SEIQRV COVID-19 associated model with the appropriate values ($\Gamma = 0.1,\ \theta = 0.15,\ \phi = 0.16,\ \gamma = 0.18,\ \eta = 0.2,\ \varphi = 0.22,\ \varsigma = 0.17,\ \mu = 0.25$):

$$\begin{cases} \left(\frac{d\mathscr{S}}{d\tau}\right) = 0.1 - 0.15\mathscr{S}\mathscr{I} + 0.02\mathscr{S}, & \mathscr{S}_0 = 0.14, \\ \left(\frac{d\mathscr{E}}{d\tau}\right) = 0.15\mathscr{S}\mathscr{I} - 0.02\mathscr{E}, & \mathscr{E}_0 = 0.16, \\ \left(\frac{d\mathscr{I}}{d\tau}\right) = 0.2\mathscr{E} - 0.57\mathscr{I}, & \mathscr{I}_0 = 0.18, \\ \left(\frac{d\mathscr{Q}}{d\tau}\right) = 0.22\mathscr{I} - 0.43\mathscr{Q}, & \mathscr{Q}_0 = 0.20, \\ \left(\frac{d\mathscr{R}}{d\tau}\right) = 0.17\mathscr{I} + 0.25\mathscr{Q} - 0.18\mathscr{R}, & \mathscr{R}_0 = 0.22, \\ \left(\frac{d\mathscr{V}}{d\tau}\right) = 0.16\mathscr{S} - 0.18\mathscr{V}, & \mathscr{V}_0 = 0.24. \end{cases} \tag{4}$$

The simulations of the SEIQRV COVID-19 linked model are numerically shown using stochastic L-MBNNs procedures requiring 11 neurons, with chosen data containing 76% in training, 10% in testing and 14% authorized. The layout of a hidden, outcome, and input neuron is shown in Fig. 3.

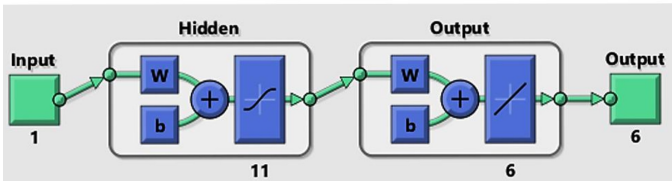

FIGURE 3. SEIQRV COVID-19 linked model solved using L-MBNNs.

Figures 4 to 6 depict the SEIQRV model based on COVID-19 by using the L-MBNNs procedures. The best results using STs are examined using the visual display in Figs. 4 and 5. The MSE and STs results of training, ideal shapes and validation are provided in Fig. 4 to solve the SEIQRV system (a to c). Depending on greatest achievements of SEIQRV scheme for epochs 20, 22 and 30, the resulting values are 5.8109×10^{-12}, 2.0758×10^{-12} and 6.9089×10^{-11}, respectively.

Overall gradient measurements are also presented in Fig. 4 (d to f) to evaluate the SEIQRV COVID-19-linked differential model using L-MBNNs. Based on the SEIQRV system's top results for epochs 20, 22 and 30, the gradient performances - for instances, 1, 2 and 3 - were found to be 8.4715×10^{-20}, 7.8693×10^{-08} and 9.2615×10^{-08}, respectively. The convergence for recommended L-MBNNs to resolve the SEIQRV COVID-19 differential model using L-MBNNs is shown in these graphical depictions.

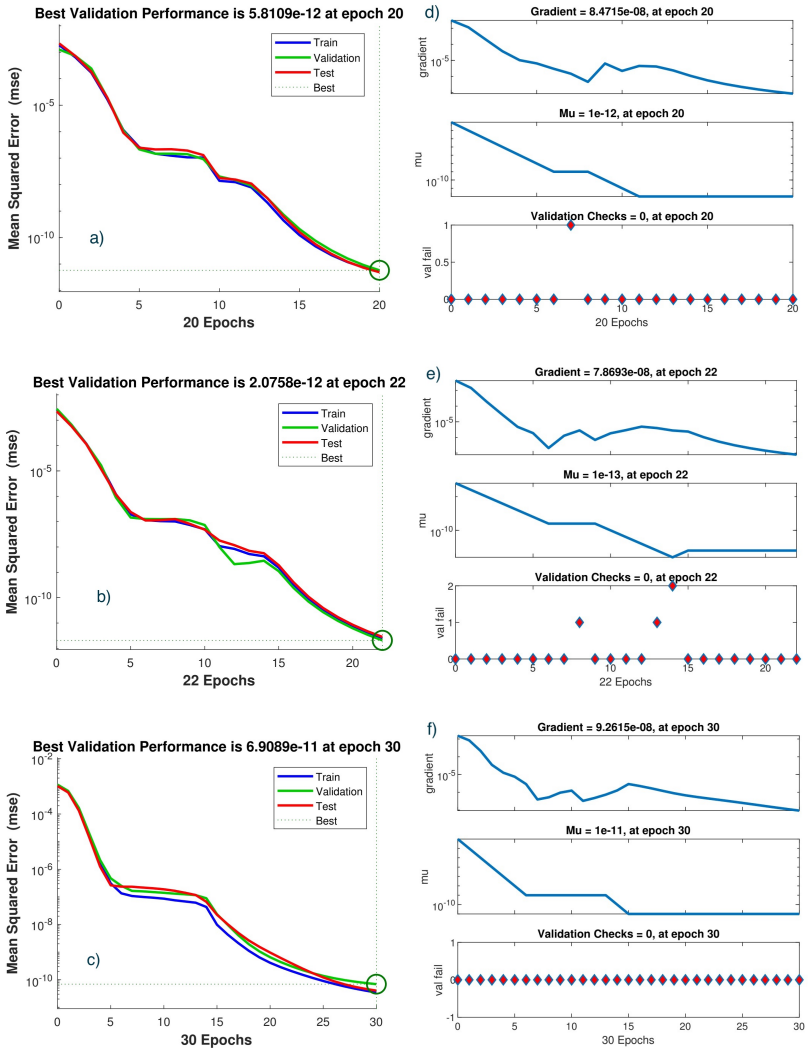

FIGURE 4. STs and MSE results used to solve the SEIQRV system.

The values of the fitted curves employed to tackle each situation for the suggested SEIQRV differentiated model are shown in Figs. 6 and 7. The effectiveness of the reference and the results obtained are compared in these visuals. The substantiation, validation and train to handle all situations of the SEIQRV COVID-19 associated differential model are shown by error graphs. Various EHs, as well as accompanying regression measures, are provided by Fig. 5 (d to f), which rely on the SEIQRV COVID-19-associated differential model (a to c). The EHs are projected to be 4.64×10^{-07}, 6.41×10^{-08} and 3.98×10^{-08}, respectively, for scenarios 1, 2 and 3.

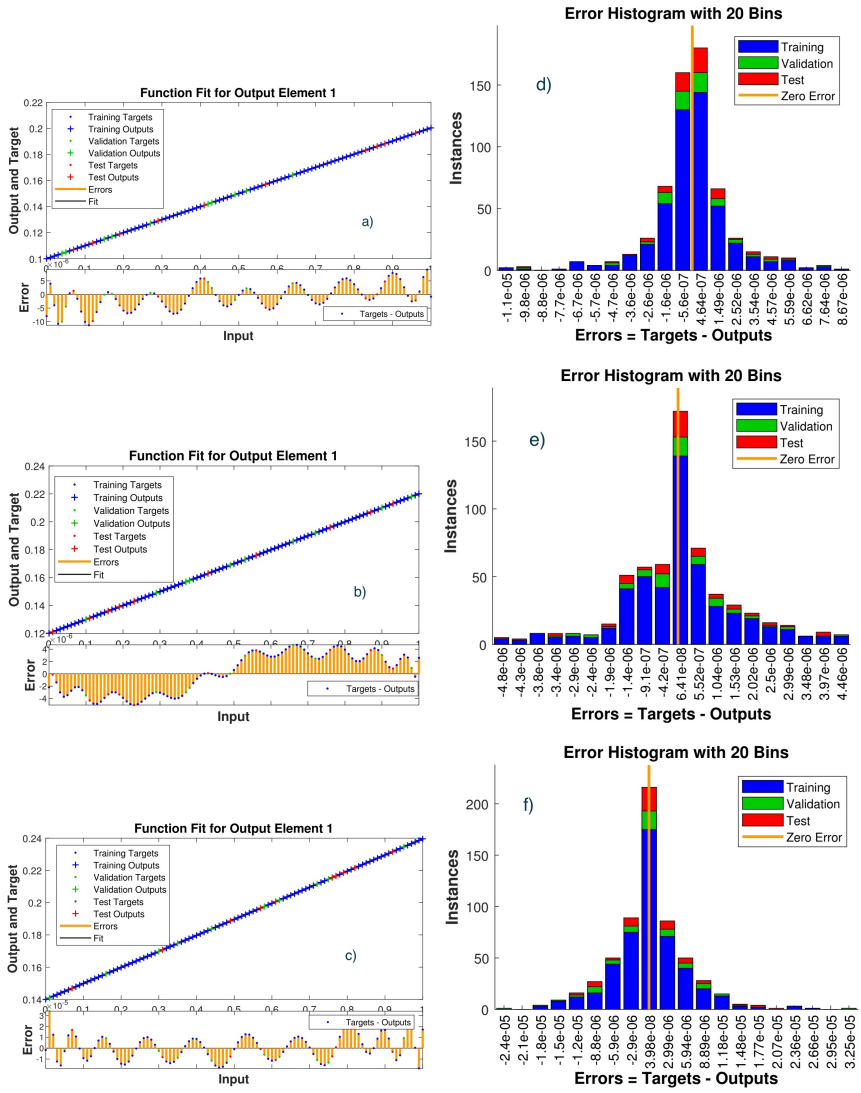

FIGURE 5. Results evaluations and EHs for the SEIQRV system.

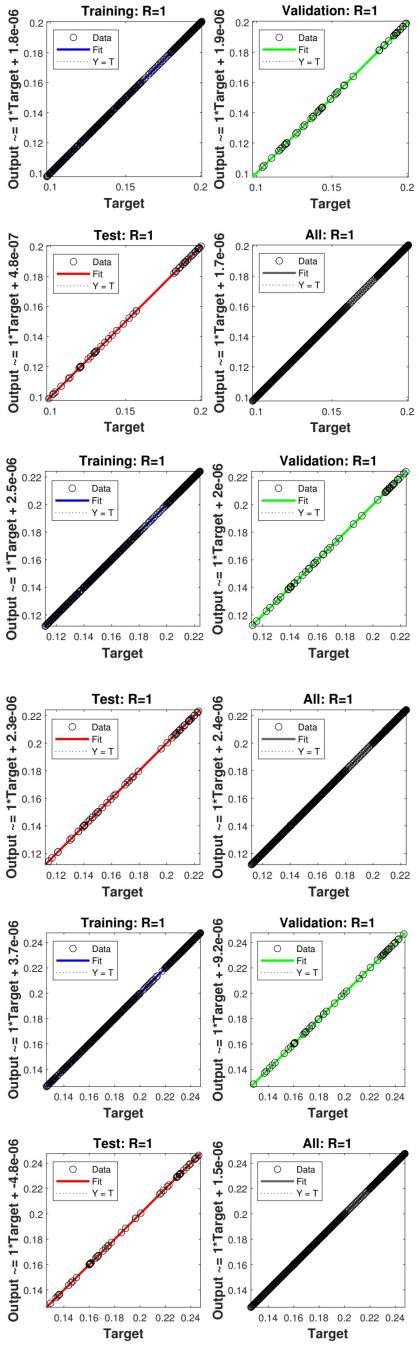

FIGURE 6. Regression plots to solve a SEIQRV system.

The association is shown in Fig. 6 to corroborate the regression's performance. The accuracy of the stochastic L-MBNNs approach to solve the fractional order SEIQRV COVID-19 differential model is demonstrated by the training, testing and authentication formulations.

Table 2 shows how the SEIQRV COVID-19-linked differential model uses MSE, complication, training, authenticate, iterations, validation and backpropagation to achieve convergence.

Table 2: The L-MBNNs approach is used to evaluate the differential model of COVID-19 SEIQRV

Case	M.S.E			Gradient	Performance	Epoch	Mu	Time
	Training	Testing	Validation					
1	5.204×10^{-12}	4.906×10^{-12}	5.810×10^{-12}	8.47×10^{-08}	5.20×10^{-12}	20	1×10^{-12}	02
2	2.518×10^{-12}	2.837×10^{-12}	2.075×10^{-12}	7.87×10^{-08}	2.52×10^{-12}	22	1×10^{-13}	02
3	3.449×10^{-11}	4.032×10^{-11}	6.908×10^{-11}	9.26×10^{-08}	3.45×10^{-11}	30	1×10^{-11}	03

Visualization for the result evaluations and also AE values are shown in Figs. 7-9 and Figs. 10-12. Numerical formulas are offered to handle the SEIQRV system using stochastic L-MBNNs. Figures 7-9 depict the consistent findings of the reference and calculated numeric outputs. The precision of L-MBNNs for resolving the SEIQRV COVID-19-linked differential model is verified by the overlapped outcome.

The AE factors used to resolve the SEIQRV COVID-19 system are shown in Fig. 10. In the dynamical range of $\mathscr{S}$, AE ratios for examples 1 to 3 are about $10^{-05} - 10^{-07}$, $10^{-05} - 10^{-06}$ and $10^{-05} - 10^{-06}$, respectively. For examples 1 to 3, AE ratios of $\mathscr{E}$ are predicted to be in a region of $10^{-06} - 10^{-08}$, $10^{-08} - 10^{-09}$, as well as $10^{-06} - 10^{-07}$. In Fig. 11, for examples 1 to 3, the AE of $\mathscr{I}$ were computed at $10^{-05} - 10^{-07}$, $10^{-06} - 10^{-07}$, as well as $10^{-05} - 10^{-06}$, respectively. Similarly, the AE for $\mathscr{Q}$ was calculated as $10^{-05} - 10^{-07}$, $10^{-06} - 10^{-07}$, and $10^{-05} - 10^{-06}$ for examples 1 to 3. Furthermore, in Fig. 12 for examples 1 to 3, the AE for $\mathscr{R}$ was calculated as $10^{-06} - 10^{-07}$, $10^{-06} - 10^{-08}$, and $10^{-05} - 10^{-07}$, respectively. The AE for $\mathscr{V}$ was calculated similarly for examples 1 to 3.

The AE results demonstrate that the L-MBNNs proposed for the SEIQRV COVID-19 scheme are successful.

The following results are based on the SEIQRV COVID19 system:

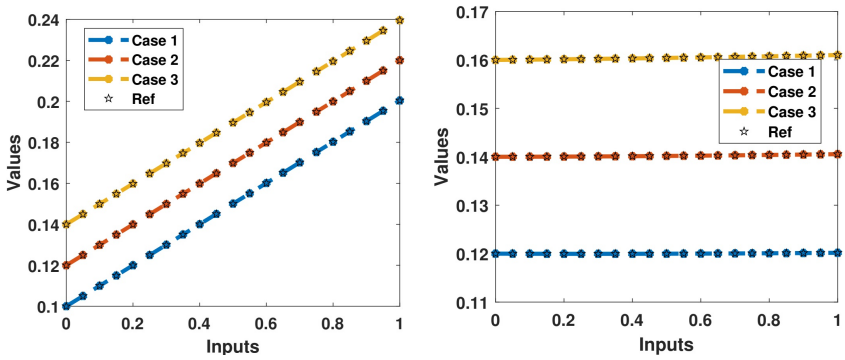

FIGURE 7. Results for $\mathscr{S}$ (left) and for $\mathscr{E}$ (right).

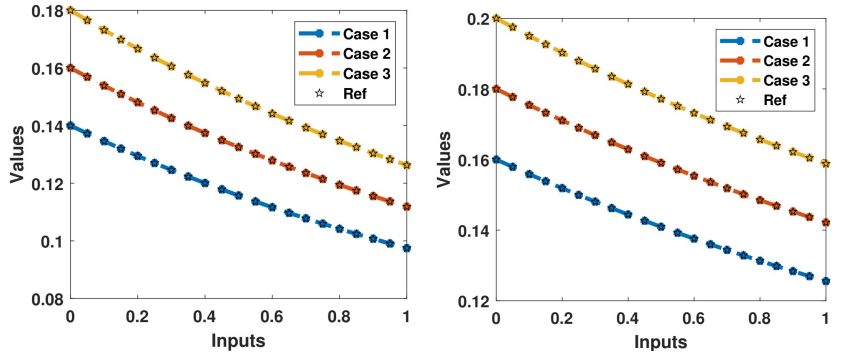

FIGURE 8. Results for $\mathscr{I}$ (left) and for $\mathscr{Q}$ (right).

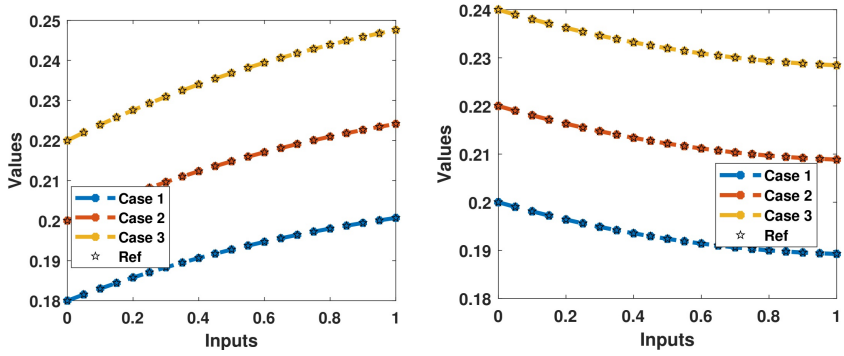

FIGURE 9. Results for $\mathscr{R}$ (left) and for $\mathscr{V}$ (right).

The absolute error is based on the SEIQRV COVID-19 system:

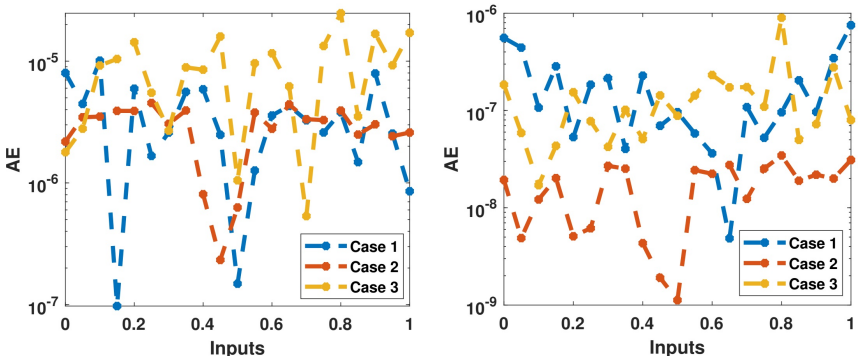

FIGURE 10. AE for $\mathscr{S}$ (left) and for $\mathscr{E}$ (right).

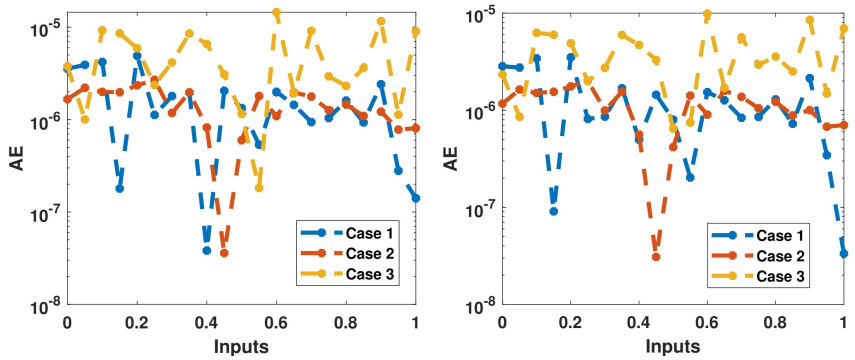

FIGURE 11. AE for $\mathscr{I}$ (left) and for $\mathscr{Q}$ (right).

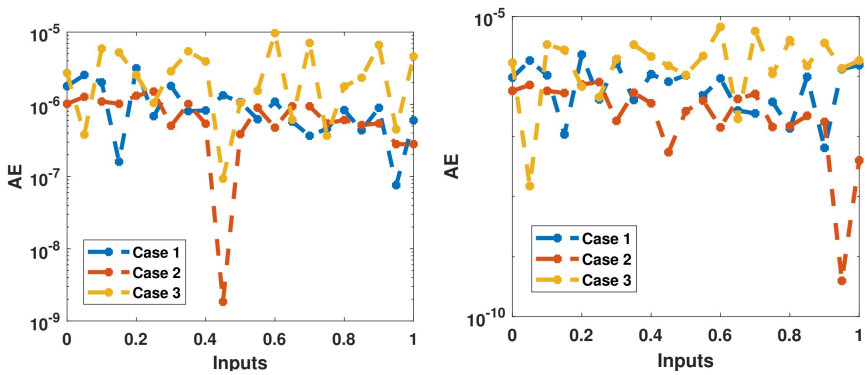

FIGURE 12. AE for $\mathscr{R}$ (left) and for $\mathscr{V}$ (right).

6. Conclusion

In this research study, a compartmental mathematical framework is used to find the numerical performances of the coronavirus dynamics along with the quarantine and vaccination impacts. The numerical stochastic process L-MBNNs has been presented to solve the model. The dynamics of the proposed model depends upon the human population that is represented by N, which is further divided into multiple subgroups. The details of these subgroups have been presented in the form of susceptible population S, exposed population E and infected people I, whereas Q represents the quarantined and R the recovered or deceased individuals. Those who have been immunized are symbolized by V. All these categories make the model SEIQRV, that is based on a system of nonlinear differential equations. The solution of this nonlinear model is proposed by the L-MBNNs. The statistics has been used to provide the numerical performances of SEIQRV model, which have been taken as 76% for training, 10% for testing and 14% for authorization. The correctness of the designed stochastic L-MBNNs procedure is obtained through the comparison of proposed and reference solutions. The reference solutions have been obtained by using the Adam method. The small value of the absolute error shows the capability of the proposed scheme. The statistical representations have been provided to check the reliability, competence and validity of L-MBNNs using different performances based on error histograms, state transitions, regression and correlation. In a future investigation the L-MBNNs might be employed to produce numerical measurement data for the Lonngren wave (Hirose and Lonngren 1985) as well as for the fluid dynamics (Vajravelu, Sreenadh, and Saravana 2017; Durur, Tasbozan, and Kurt 2020; İlhan and Kıymaz 2020).

Author contributions

Conceptualization: Z.S., M.A.Z.R. and H.M.B.; methodology: Z.S., M.A.Z.R. and H.M.B.; writing and editing: Z.S., M.A.Z.R., H.M.B. and A.C.; investigation: Z.S., M.A.Z.R., H.M.B. and A.C.; mathematical model: A.C. All authors have read and agreed to the published version of the manuscript.

Acknowledgments

This work was supported by the *Gruppo Nazionale per la Fisica Matematica* of the *Istituto Nazionale di Alta Matematica* (GNFM-INDAM), Italy.

References

Agusto, F. B. and Khan, M. A. (2018). "Optimal control strategies for dengue transmission in pakistan". *Mathematical Biosciences* **305**, 102–121. DOI: 10.1016/j.mbs.2018.09.007.

Ahmad, W. M. and El-Khazali, R. (2007). "Fractional-order dynamical models of love". *Chaos, Solitons & Fractals* **33**(4), 1367–1375. DOI: 10.1016/j.chaos.2006.01.098.

Ahmad, Z., Ali, F., Khan, N., and Khan, I. (2021). "Dynamics of fractal-fractional model of a new chaotic system of integrated circuit with Mittag-Leffler kernel". *Chaos, Solitons & Fractals* **153**, 111602. DOI: 10.1016/j.chaos.2021.111602.

Ahmad, Z., Arif, M., Ali, F., Khan, I., and Nisar, K. S. (2020a). "A report on COVID-19 epidemic in Pakistan using SEIR fractional model". *Scientific Reports* **10**(1). DOI: 10.1038/s41598-020-79405-9.

Ahmad, Z., Khan, N., Arif, M., Murtaza, S., and Khan, I. (2020b). "Dynamics of fractional order SIR model with a case study of COVID-19 in Turkey". *International Journal of Computational Analysis* **4**(1), 18–35. URL: https://cuijca.com/ojs/index.php/ijca/article/view/43.

Ali, F., Ahmad, Z., Arif, M., Khan, I., and Nisar, K. S. (2020). "A time fractional model of generalized Couette flow of couple stress nanofluid with heat and mass transfer: Applications in engine oil". *IEEE Access* **8**, 146944–146966. DOI: 10.1109/ACCESS.2020.3013701.

Amawi, H., Deiab, G. I. A., Aljabali, A. A. A., Dua, K., and Tambuwala, M. M. (2020). "COVID-19 pandemic: an overview of epidemiology, pathogenesis, diagnostics and potential vaccines and therapeutics". *Therapeutic Delivery* **11**(4), 245–268. DOI: 10.4155/tde-2020-0035.

Ao, S., Han, D., Sun, L., Wu, Y., Liu, S., and Huang, Y. (2020). "Identification of potential key agents for targeting RNA-dependent RNA polymerase of SARS-CoV-2 by integrated analysis and virtual drug screening". *Frontiers in Genetics* **11**. DOI: 10.3389/fgene.2020.581668.

Atangana, A. (2017). "Fractal-fractional differentiation and integration: Connecting fractal calculus and fractional calculus to predict complex system". *Chaos, Solitons & Fractals* **102** (Future Directions in Fractional Calculus Research and Applications), 396–406. DOI: 10.1016/j.chaos.2017.04.027.

Brauer, F. (2017). "Mathematical epidemiology: Past, present, and future". *Infectious Disease Modelling* **2**(2), 113–127. DOI: 10.1016/j.idm.2017.02.001.

Ciancio, A., Ciancio, V., and Flora, B. F. F. (2023). "A fractional rheological model of viscoanelastic media". *Axioms* **12**(3), 243. DOI: 10.3390/axioms12030243.

Ciancio, A. and Flora, B. F. F. (2017). "A fractional complex permittivity model of media with dielectric relaxation". *Fractal and Fractional* **1**(1), 4. DOI: 10.3390/fractalfract1010004.

Durur, H., Tasbozan, O., and Kurt, A. (2020). "New analytical solutions of conformable time fractional bad and good modified Boussinesq equations". *Applied Mathematics and Nonlinear Sciences* **5**(1), 447–454. DOI: 10.2478/amns.2020.1.00042.

Ghanbari, B. and Djilali, S. (2020). "Mathematical analysis of a fractional-order predator-prey model with prey social behavior and infection developed in predator population". *Chaos, Solitons & Fractals* **138**, 109960. DOI: 10.1016/j.chaos.2020.109960.

Guirao, J. L. G., Sabir, Z., and Saeed, T. (2020). "Design and numerical solutions of a novel third-order nonlinear Emden-Fowler delay differential model". *Mathematical Problems in Engineering*, 7359242 (Recent Trends in Special Functions and Analysis of Differential Equations). DOI: 10.1155/2020/7359242.

Hirose, A. and Lonngren, K. E. (1985). *Introduction to Wave Phenomena*. New York, NY: Wiley.

İlhan, E. and Kıymaz, İ. O. (2020). "A generalization of truncated M-fractional derivative and applications to fractional differential equations". *Applied Mathematics and Nonlinear Sciences* **5**(1), 171–188. DOI: 10.2478/amns.2020.1.00016.

Kantner, M. and Koprucki, T. (2020). "Beyond just "flattening the curve": Optimal control of epidemics with purely non-pharmaceutical interventions". *Journal of Mathematics in Industry* **10**(1), 23. DOI: 10.1186/s13362-020-00091-3.

Khan, M. A. and Atangana, A. (2019). "Dynamics of Ebola disease in the framework of different fractional derivatives". *Entropy* **21**(3), 303. DOI: 10.3390/e21030303.

Khan, N., Ali, F., Arif, M., Ahmad, Z., Aamina, A., and Khan, I. (2021). "Maxwell nanofluid flow over an infinite vertical plate with ramped and isothermal wall temperature and concentration". *Mathematical Problems in Engineering*, 3536773. DOI: 10.1155/2021/3536773.

Kumar, A., Dwivedi, P., Kumar, G., Narayan, R. K., Jha, R., Parashar, R., Sahni, C., and Pandey, S. N. (2021). "Second wave of COVID-19 in India could be predicted with genomic surveillance of SARS-CoV-2 variants coupled with epidemiological data: A tool for future". *medRxiv*, 2021.06.09.21258612. DOI: 10.1101/2021.06.09.21258612.

Martcheva, M. (2015). "Introduction to Epidemic Modeling". In: *An introduction to Mathematical Epidemiology*. Vol. 61. Texts in Applied Mathematics. Boston, MA: Springer US, pp. 9–31. DOI: 10.1007/978-1-4899-7612-3_2.

Peter, O. J., Qureshi, S., Yusuf, A., Al-Shomrani, M., and Idowu, A. A. (2021). "A new mathematical model of COVID-19 using real data from Pakistan". *Results in Physics* **24**, 104098. DOI: 10.1016/j.rinp.2021.104098.

Qureshi, S. and Jan, R. (2021). "Modeling of measles epidemic with optimized fractional order under Caputo differential operator". *Chaos, Solitons & Fractals* **145**, 110766. DOI: 10.1016/j.chaos.2021.110766.

Sabir, Z., Guirao, J. L. G., and Saeed, T. (2021). "Solving a novel designed second order nonlinear Lane–Emden delay differential model using the heuristic techniques". *Applied Soft Computing* **102**, 107105. DOI: 10.1016/j.asoc.2021.107105.

Sabir, Z., Raja, M. A. Z., Alnahdi, A. S., Jeelani, M. B., and Abdelkawy, M. A. (2022). "Numerical investigations of the nonlinear smoke model using the Gudermannian neural networks". *Mathematical Biosciences and Engineering* **19**(1), 351–370. DOI: 10.3934/mbe.2022018.

Sabir, Z., Raja, M. A. Z., Guirao, J. L. G., and Saeed, T. (2021a). "Meyer wavelet neural networks to solve a novel design of fractional order pantograph Lane-Emden differential model". *Chaos, Solitons & Fractals* **152**, 111404. DOI: 10.1016/j.chaos.2021.111404.

Sabir, Z., Raja, M. A. Z., Guirao, J. L. G., and Shoaib, M. (2020). "A neuro-swarming intelligence-based computing for second order singular periodic non-linear boundary value problems". *Frontiers in Physics* **8**. DOI: 10.3389/fphy.2020.00224.

Sabir, Z., Wahab, H. A., Javeed, S., and Baskonus, H. M. (2021b). "An efficient stochastic numerical computing framework for the nonlinear higher order singular models". *Fractal and Fractional* **5**(4), 176. DOI: 10.3390/fractalfract5040176.

Sharomi, O. and Malik, T. (2017). "Optimal control in epidemiology". *Annals of Operations Research* **251**(1), 55–71. DOI: 10.1007/s10479-015-1834-4.

Sinan, M., Shah, K., Kumam, P., Mahariq, I., Ansari, K. J., Ahmad, Z., and Shah, Z. (2022). "Fractional order mathematical modeling of typhoid fever disease". *Results in Physics* **32**, 105044. DOI: 10.1016/j.rinp.2021.105044.

Song, L., Xu, S., and Yang, J. (2010). "Dynamical models of happiness with fractional order". *Communications in Nonlinear Science and Numerical Simulation* **15**(3), 616–628. DOI: 10.1016/j.cnsns.2009.04.029.

Ullah, S., Khan, M. A., and Farooq, M. (2018). "A fractional model for the dynamics of TB virus". *Chaos, Solitons & Fractals* **116**, 63–71. DOI: 10.1016/j.chaos.2018.09.001.

Umakanthan, S., Sahu, P., Ranade, A. V., Bukelo, M. M., Rao, J. S., Abrahao-Machado, L. F., Dahal, S., Kumar, H., and Dhananjaya, K. V. (2020). "Origin, transmission, diagnosis and management of coronavirus disease 2019 (COVID-19)". *Postgraduate Medical Journal* **96**(1142), 753–758. URL: https://pmj.bmj.com/content/96/1142/753.

Vajravelu, K., Sreenadh, S., and Saravana, R. (2017). "Influence of velocity slip and temperature jump conditions on the peristaltic flow of a Jeffrey fluid in contact with a Newtonian fluid". *Applied Mathematics and Nonlinear Sciences* **2**(2), 429–442. DOI: 10.21042/AMNS.2017.2.00034.

Yüce, M., Filiztekin, E., and Özkaya, K. G. (2021). "COVID-19 diagnosis – A review of current methods". *Biosensors and Bioelectronics* **172**, 112752. DOI: 10.1016/j.bios.2020.112752.

[a] Hazara University,
Department of Mathematics and Statistics,
Mansehra, Pakistan
and
Lebanese American University,
Department of Computer Science and Mathematics,
Beirut, Lebanon

[b] National Yunlin University of Science and Technology,
Future Technology Research Center,
123 University Road, Section 3, Douliou, Yunlin 64002, Taiwan

[c] Harran University,
Department of Mathematics and Science Education, Faculty of Education,
Sanliurfa, Turkey

[d] Università degli Studi di Messina,
Dipartimento di Scienze Biomediche, Odontoiatriche e delle Immagini Morfologiche e Funzionali,
Messina, Italy

[*] To whom correspondence should be addressed | email: aciancio@unime.it

Communicated 24 May 2022; manuscript received 11 June 2022; published online 12 May 2023